

**Development and Evaluation of the Advanced Pedestrian Legform Impactor Prototype  
which can be Applicable to All Types of Vehicles Regardless of Bumper Height  
- Part 2: Actual Test Tool -**

Atsuhiko Konosu, Takahiro Isshiki, Yukou Takahashi

**Abstract**

In our preceding study, we developed an advanced pedestrian legform impactor prototype FE model which can be applicable to all types of vehicles regardless of the bumper height without any change of impact height from that of human. In addition, we also considered the technical feasibility to develop an actual test tool based on the specification of the aPLI PT FE model. However, no one had developed an actual test tool based on the specifications of the FE model, therefore, it was unclear that the existence of technical feasibility to fabricate an actual test tool based on the aPLI PT FE model as well as to conduct a free flight test.

In this study, therefore, we developed an advanced pedestrian legform impactor prototype actual test tool based on its FE model to confirm the technical feasibility to fabricate it as well as to conduct a free flight test using it without any issues. In addition, we evaluated its biofidelity based on the free flight test data.

As a result, we confirmed that no serious technical feasibility issues exist, furthermore, we confirmed its high biofidelity under free flight test conditions against low-bumper and high-bumper actual simplified vehicles.

**Keywords** influences of the upper body, legform impactor, pedestrian protection test method, computer simulation.

## I. INTRODUCTION

In our preceding study [1], we developed an advanced pedestrian legform impactor prototype (aPLI PT) FE model, as shown in Figure 1, which can be applied to any types of vehicle by improving specifications of the flexible pedestrian legform impactor as well as by adding a biofidelic simplified upper body part. In addition, we considered the technical feasibility to develop an actual test tool based on the specification of the aPLI PT FE model.

We confirmed its high biofidelity by the comparison of injury measures between the aPLI PT FE model and a well validated human full-body finite element model quantitatively under the collisions with 18 types low-bumper and 18 types high-bumper simplified vehicles. Contrary, no one had confirmed the technical feasibility to fabricate an aPLI PT actual test tool based on the specifications of its FE model as well as the technical feasibility to conduct a free flight test using it. In addition, the high biofidelity of the actual test tool is uncertain.

In this study, we developed the aPLI PT actual test tool based on the specifications of its FE model in order to confirm the technical feasibility to fabricate it as an actual test tool as well as the technical feasibility to conduct free flight tests using it. In addition, we confirmed its biofidelity under a free flight test condition against a low-bumper and a high-bumper actual simplified vehicle.

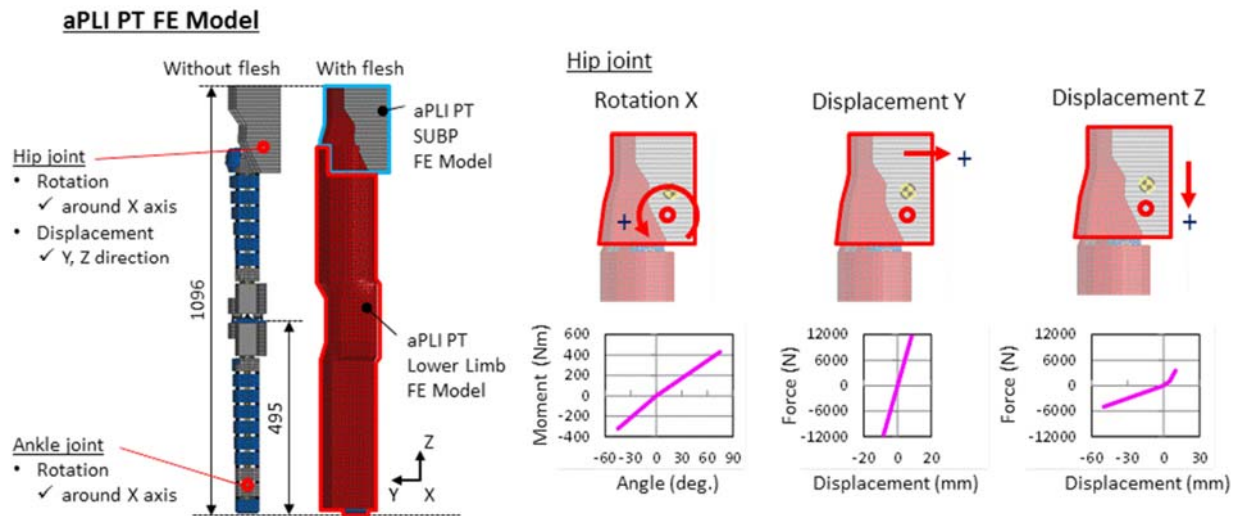


Fig. 1. Overview of the aPLI PT FE model.

## II. METHODS

### **Development Methods of the aPLI PT Actual Test Tool**

**Construction:** The aPLI PT actual test tool was developed based on the specifications of its FE model. The aPLI PT actual test tool consists of a SUBP part and a lower limb part.

Figure 2 and Figure 3 show an overview of the SUBP part of the aPLI PT actual test tool. It consists of a main body (Figure 2) and flesh (Figure 3). The main body has a steel housing to simulate the rigid stiffness of its FE model. Its mass, moment of inertia, and position of center of gravity are comparable to its FE model. The hip joint installed in the main body is made by a mechanical rotational and translational joint which has joint characteristics based on the compression stiffness of the urethane springs. The flesh is made by a construction of laminating neoprene sheets to simulate that of the FE model.

Figure 4 and Figure 5 show an overview of the lower limb part of the aPLI PT actual test tool. It consists of a main body (Figure 4) and flesh (Figure 5). The main body has similar construction and mass to that of its FE model. The geometric layout of the anterior cruciate ligament (ACL) and the posterior cruciate ligament (PCL) is made vertical as is that of the FE model. The femur bone core width and shape of the impact surface are comparable to that of its FE model. With regard to the ankle joint, it was made by a mechanical rotational joint with free movement. The main body is attached to the SUBP part by having femoral offset, as has the FE model.

For the flesh part, several pieces of lead were attached by glue to the side of the flesh to make it as heavy as its FE model. In addition, several holes were made in the back of the flesh so the parts are exposed, allowing the long bones to be pushed directly with a launcher, i.e. not to be pushed via the flesh as with the FlexPLI.

Figure 6 shows an overview of the aPLI PT actual test tool in an assembled condition. The aPLI PT actual test tool has a larger size and mass compared to that of the FlexPLI actual test tool due to the addition of the SUBP part.

**Measurements:** With regards to the measurement sensors, we basically kept all sensors of the FlexPLI as shown in Figure 7. In addition, three Angular Rate Sensors (ARS) were attached to the SUBP part of the aPLI PT actual test tool in order to check the attitude during the free flight before the impact to a vehicle, as shown in Figure 8. Contrary, two ARS sensors (y and z) were removed from at the knee joint of the lower limb part because the measurement values from those sensors are the same of those of the SUBP part, i.e. the SUBP and lower limb are fixed tight to each other around the y and z axis, so they rotate together. Three accelerometers were attached to the SUBP part as references.

The Data Acquisition System (DAS) was installed in the free space of the SUBP part of the aPLI PT actual test tool as shown in Figure 8. In the case of the FlexPLI, the DAS is installed at the knee joint. However, we changed

the installment position to allow for easy access to the DAS, as well as to allow much free space compared to the knee joint.

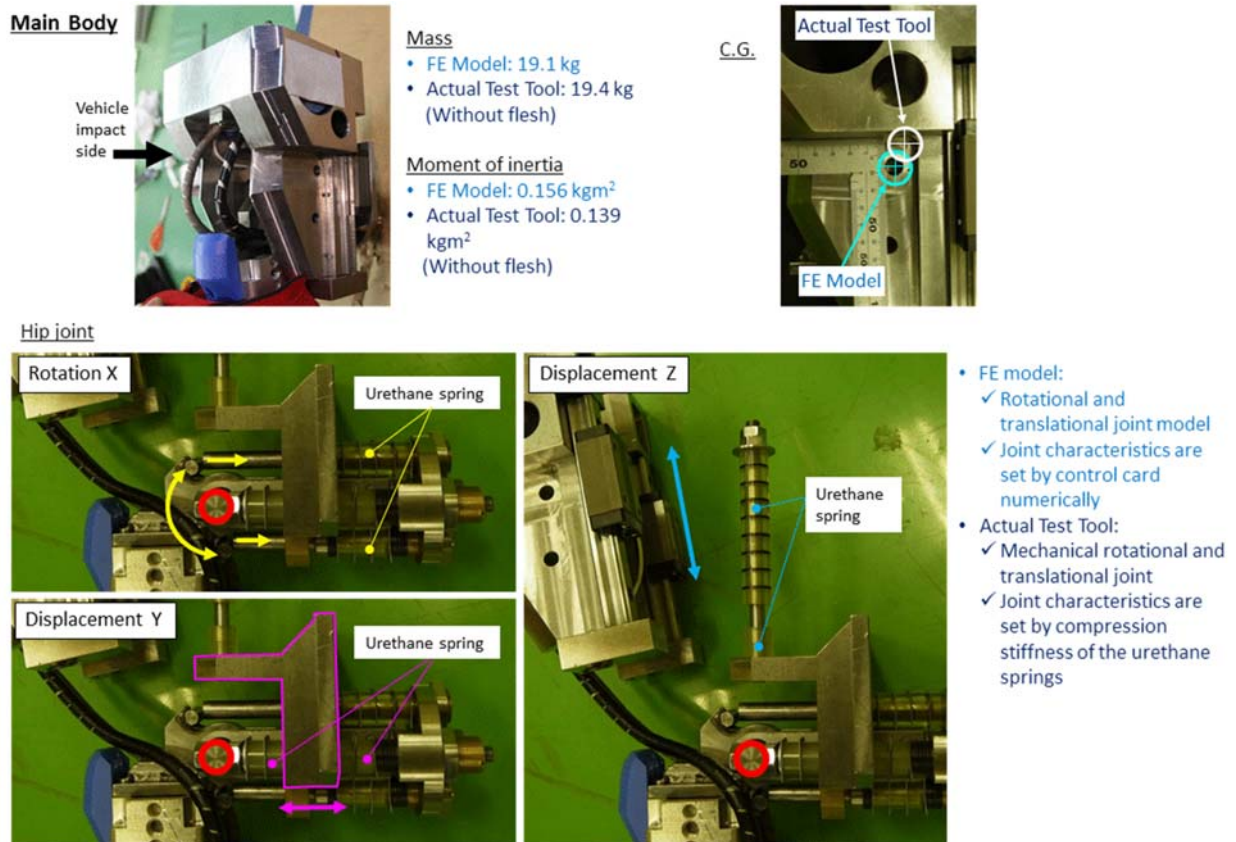


Fig. 2. Overview of the SUBP part of the aPLI PT actual test tool (main body).



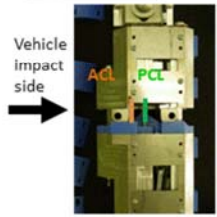
Fig. 3. Overview of the SUBP part of the aPLI PT actual test tool (flesh).

**Main Body**

Mass

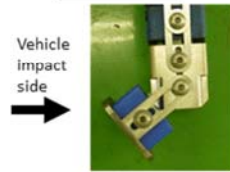
- FE Model: 6.8 kg
- Actual Test Tool: 6.6 kg

Geometric layout of the ACL and the PCL



- FE model:
  - ✓ Vertical layout
- Actual Test Tool:
  - ✓ same as above

Representation of the ankle joint



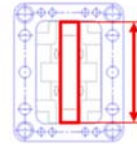
- FE model:
  - ✓ Rotational joint model with free rotation
- Actual Test Tool:
  - ✓ Mechanical rotational joint with free rotation

Femoral offset



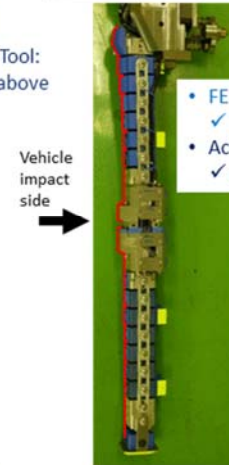
- FE model:
  - ✓ 40 mm
- Actual Test Tool:
  - ✓ same as above

Femur bone core



- FE model: 55 mm
- Actual Test Tool: same as above

Shape of the impact surface of the long bones



- FE model:
  - ✓ Non-Flat
- Actual Test Tool:
  - ✓ same as above

Fig. 4. Overview of the lower limb part of the aPLI PT actual test tool (main body).

**Flesh**

Flesh outer



Flesh inner

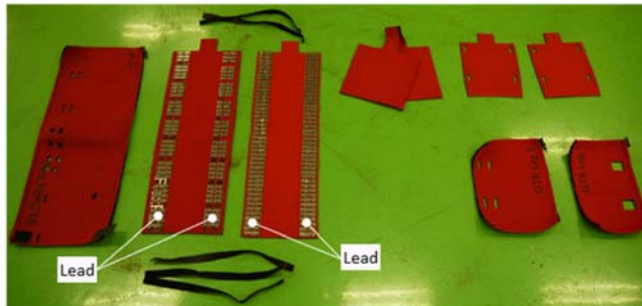


Mass

- FE Model: 6.1 kg
- Actual Test Tool: 6.3 kg

Structure

- FE model
  - ✓ Laminating structure of the neoprene sheets
  - ✓ High density is applied to the model
- Actual Test Tool
  - ✓ Laminating structure of the neoprene sheets
  - ✓ Several pieces of lead were attached by glue to the side of the flesh to make flesh as heavy as that of the FE model



○ Holes for pushing parts to push long bones directly by launcher (not via flesh)

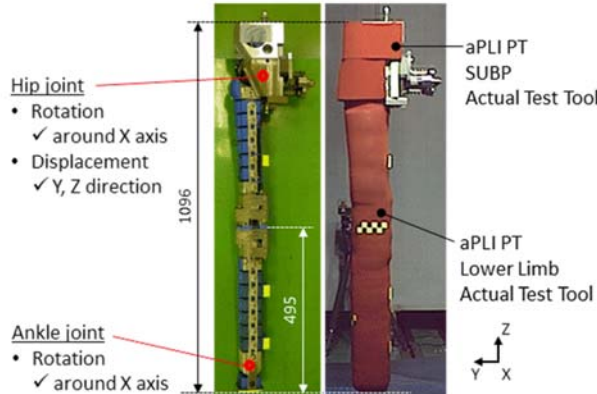
Fig. 5. Overview of the lower limb part of the aPLI PT actual test tool (flesh).

**aPLI PT Actual Test Tool**

Mass

- 32.3 kg (with flesh)

Without flesh      With flesh



Hip joint

- Rotation
  - ✓ around X axis
- Displacement
  - ✓ Y, Z direction

Ankle joint

- Rotation
  - ✓ around X axis

**Flex PLI Actual Test Tool**

Mass

- 13.1 kg (with flesh)

Without flesh      With flesh

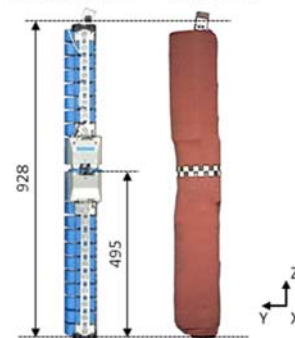


Fig. 6. Overview of the aPLI PT actual test tool (assembled condition).

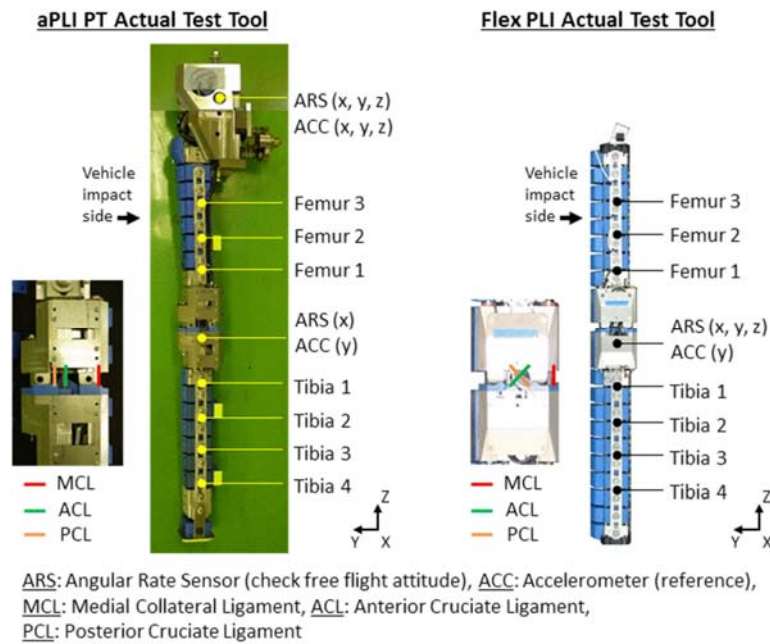


Fig. 7. Measurement Items of the aPLI PT actual test tool.

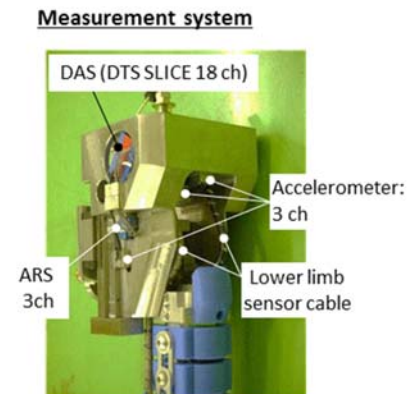


Fig. 8. Measurement Items and DAS system at the SUBP part of the aPLI PT actual test tool.

**Evaluation Methods of the aPLI PT Actual Test Tool**

Performance of the component levels of the aPLI PT actual test tool were evaluated by conducting loading tests at the femur, tibia, knee, and hip joint respectively as shown in Table 1.

After the component level loading tests, we evaluated its technical feasibility issues such as durability and free flight attitude and vibration as well as biofidelity under free flight tests by using two types of actual simplified vehicles (high-bumper type and low-bumper type) as shown in Figure 9. Those simplified vehicles can demonstrate upper body influence on the load at the lower limb under the low-bumper and high-bumper impact respectively (Appendix Figure A-1 and Figure A-2). In the low-bumper impact, the human lower limb FE model and the FlexPLI FE model have a larger lean down phenomenon compared to that of the human full-body model (Figure A-1). Contrary, in the high-bumper impact, for the human lower limb FE model and the FlexPLI FE model significant rebound phenomenon are observed compared to that of the human full-body model (Figure A-2). Biofidelity of the aPLI PT actual test tool was evaluated by comparing kinematics as well as injury measures with that of the human full-body FE model and the FlexPLI FE model.

TABLE I  
GENERAL INFORMATION FOR THE COMPONENT TEST APPLIED TO THE APLI PT ACTUAL TEST TOOL

Test type	Evaluation items	Image	Test type	Evaluation items	Image
<u>Femur and Tibia 3-point bending test</u> • n= 3 for each	Displacement - Moment		<u>Hip joint mobility test</u> • Rotation x (n= 2) • Displacement y (n= 2) • Displacement z (n= 2)	Displacement - Force Angle - Moment	
<u>Knee 3-point bending test</u> • n= 3	Erongation - Moment/Force				

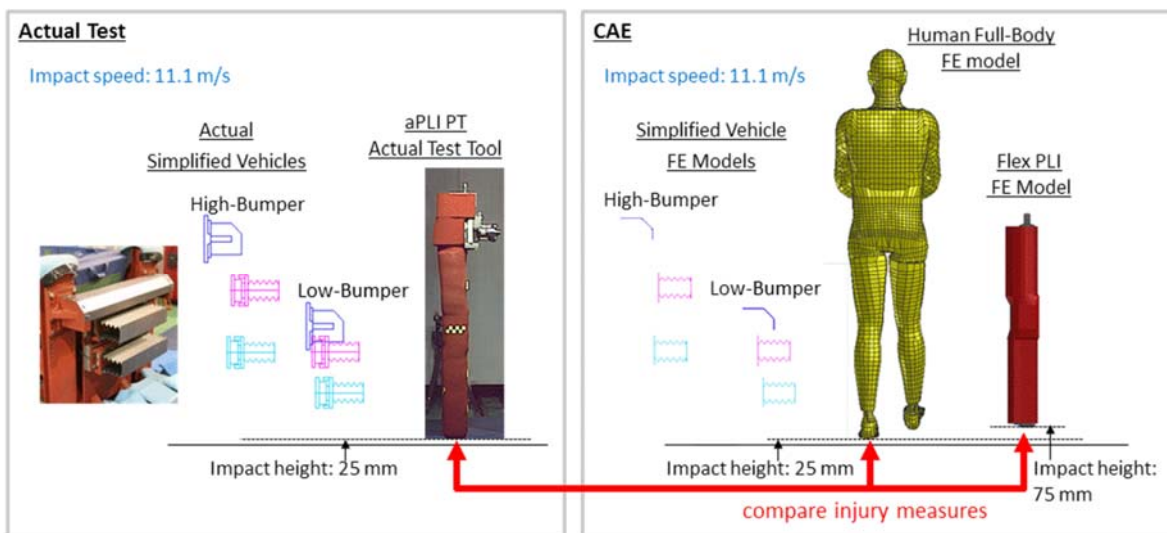


Fig. 9. Overview of the evaluation test method for the aPLI PT actual test tool (biofidelity and technical issues).

### III. RESULTS

#### Evaluation Results of the aPLI PT Actual Test Tool

*Component Test Results* Figure 10 to Figure 12 show component test results of the femur, tibia, knee, and hip joint of the developed aPLI PT actual test tool. Each response to the loads of the femur, tibia, and knee shows high correlation with that of the FE model. On the other hand, the hip joint shows some differences especially for the rotation x (plus and minus) and displacement z (minus). Joint characteristics for the rotation x is softer than that of the FE model, and the joint characteristic for the displacement z (minus) shows a bottoming out phenomenon after the -30 mm deflection. The difference for rotation x (plus and minus) joint characteristic is caused by the relatively soft urethane springs stiffness to simulate that of the FE model. The difference for the displacement z (minus) joint characteristic is caused by the urethane springs becoming stuck because of large deformation as shown in Figure 13.

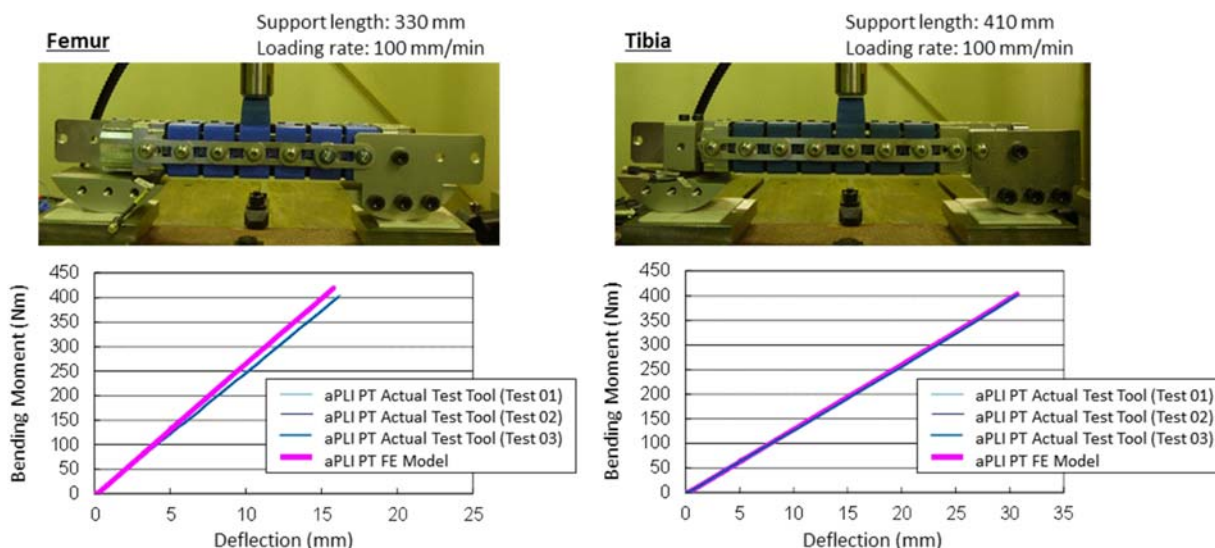


Fig. 10. Component test results of the aPLI PT actual test tool (femur and tibia).

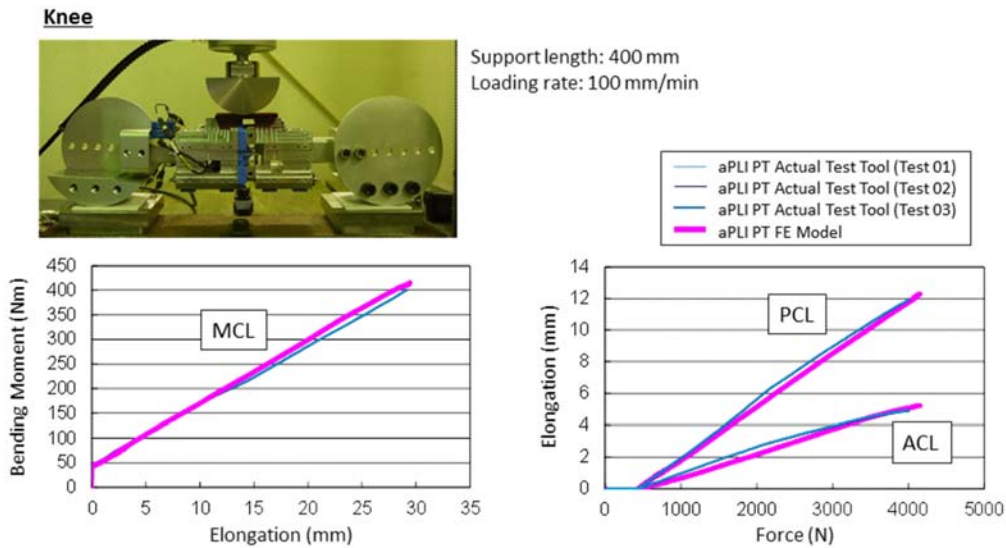


Fig. 11. Component test results of the aPLI PT actual test tool (knee).

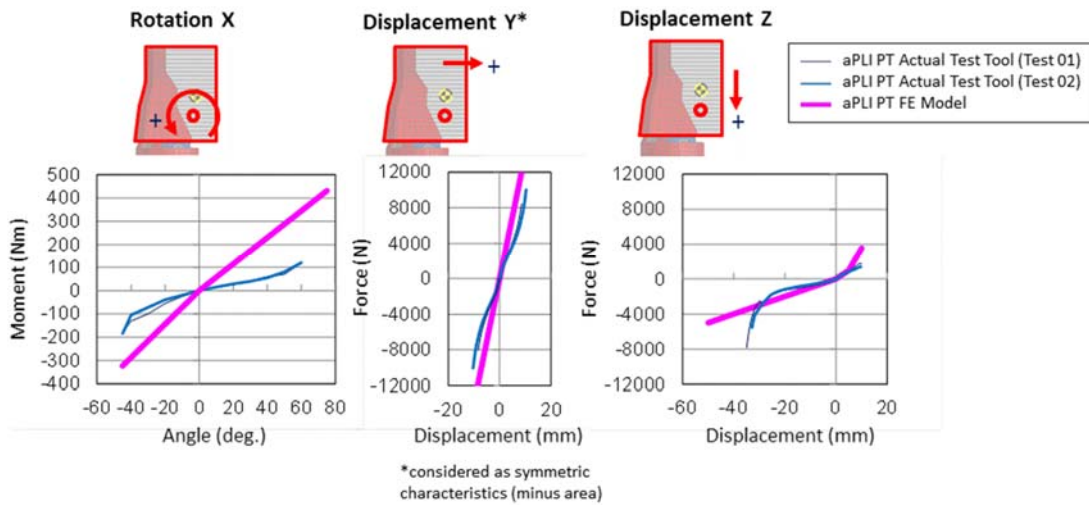


Fig. 12. Component test results of the aPLI PT actual test tool (hip joint).

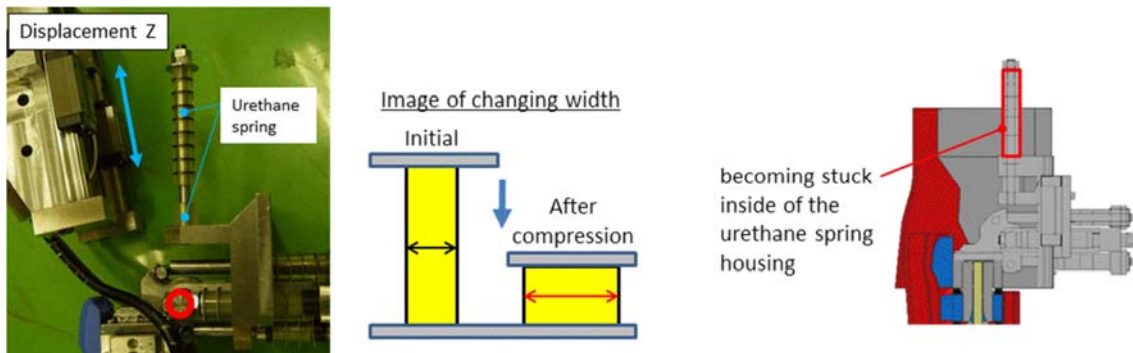


Fig. 13. Schematic explanation of the urethane spring stuck phenomenon.

*Simplified Actual Vehicle Test Results* We conducted three tests for the low-bumper type actual simplified vehicle and three tests for the high-bumper type actual simplified vehicle as shown in Table 2. Those tests were conducted within the requirements of free flight test conditions (impact speed, temperature, humidity, and impact location) settled in the amendment of Regulation No. 127 of the United Nations (UN-R127 Amendment) [2].

In the testing, we observed no technical issues with regards to free flight attitude and vibration as shown in Table 3. Requirement of the free flight attitude and vibration are referred to the UN-R127 Amendment. Furthermore, no technical issues occurred with regard to the durability of the aPLI PT actual test tool during the test.

Figure 14 and Figure 15 show free flight test results of the aPLI PT actual test tool for the low-bumper type actual simplified vehicle. The aPLI actual test tool shows a comparable response with the human full-body FE model. On the contrary, the FlexPLI FE model shows a larger lean down phenomenon of the femur compared to the aPLI actual test tool and human full-body FE model. With regard to the time historical injury measure data, the aPLI PT actual test tool are also more comparable to that of the human full-body FE model compared to that of the FlexPLI FE model. Especially, the aPLI PT actual test tool does not show any non-biofidelic two peak waveforms at the tibia as generated in the FlexPLI FE model.

Figure 16 and Figure 17 show free flight test results of the aPLI PT actual test tool for the high-bumper type actual simplified vehicle. The aPLI actual test tool shows a comparable response with the human full-body FE model. On the contrary, the FlexPLI FE model shows significant rebound phenomenon of the femur compared to that of the aPLI actual test tool and the human full-body FE model. With regard to the time historical injury measure data of the aPLI PT actual test tool are also more comparable to that of the human full-body FE model compared to that of the FlexPLI FE model especially for the femur because of having the aPLI PT SUBP part which can simulate upper body influence to the load of the lower limb appropriately.

TABLE II  
TEST CONDITIONS FOR THE SIMPLIFIED ACTUAL SIMPLIFIED VEHICLE

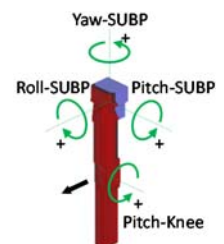
Test ID	Simplified Vehicle Type	Impact Speed (m/s)	Temperature (°C)	Humidity (%)	Location* (mm)
Test01	Low-bumper	11.04	20.4	44	L4
Test02	Low-bumper	11.13	20.5	48	R1, D3
Test03	Low-bumper	11.11	20.3	50	R1
Test04	High-bumper	11.10	20.0	55	L2
Test05	High-bumper	11.11	20.2	57	L4, D2
Test06	High-bumper	11.13	20.3	57	L2, D5
Requirements		11.1±0.2	20±4	40±30	±10

\* L: left, R: right, D: down

Requirement Pass Fail

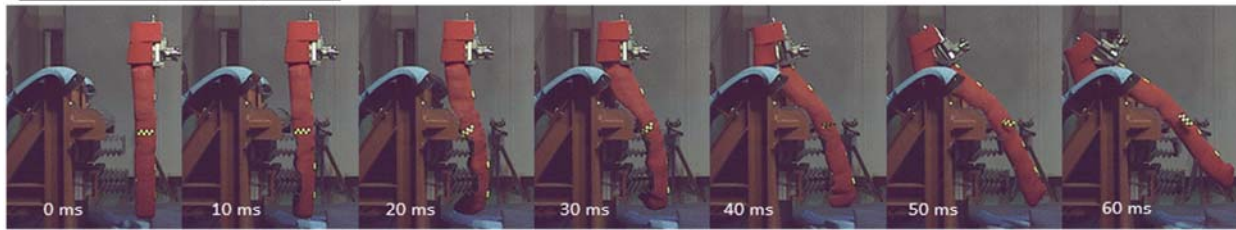
TABLE A- III  
TEST CONDITIONS FOR THE SIMPLIFIED ACTUAL SIMPLIFIED VEHICLE

Item		Test 01	Test 02	Test 03	Test 04	Test 05	Test 06	Requirements
Attitude	Roll-SUBP (deg.)	-0.7	-0.6	-0.7	-1.3	-1.3	-0.6	±2
	Yaw-SUBP (deg.)	-0.1	0.1	-0.5	0	-0.1	-0.1	±2
	Pitch-SUBP (deg.)	-1.3	-1.8	-1.6	-1.1	-1.7	-1.1	±2
	Pitch-Knee (deg.)	-0.2	-0.8	-0.6	-0.5	-0.2	-0.6	±2
Vibration	Femur 3 (Nm)	1.2	-2.4	-1.6	-3.6	-2.1	-1	±10
	Femur 2 (Nm)	0.3	-3.5	-1.9	-4.2	-0.8	-1.4	±10
	Femur 1 (Nm)	-1.5	-6.1	-4.2	-5.1	-5.3	-1.4	±10
	Tibia 1 (Nm)	-3.3	-7.1	-6	-3	0	1.4	±10
	Tibia 2 (Nm)	-4	-5.7	-5.9	-2.3	-0.2	1.1	±10
	Tibia 3 (Nm)	-3.4	-4	-4.2	-2.1	-0.5	0.7	±10
	Tibia 4 (Nm)	-1.6	-3.2	-3.1	-1.2	-0.5	0.1	±10

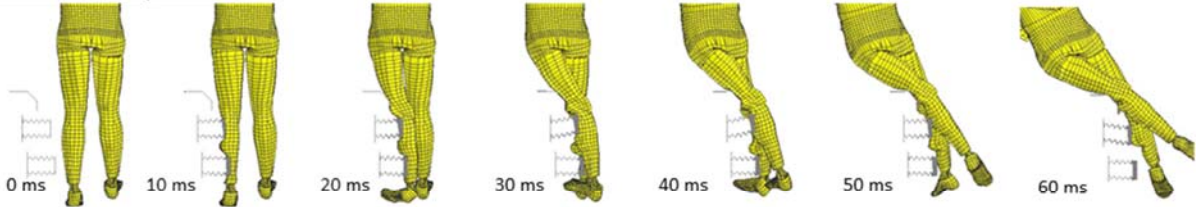


Requirement Pass Fail

**aPLI PT Actual Test Tool (Test 01)**



**Human Full-Body FE Model**



**Flex PLI FE Model**

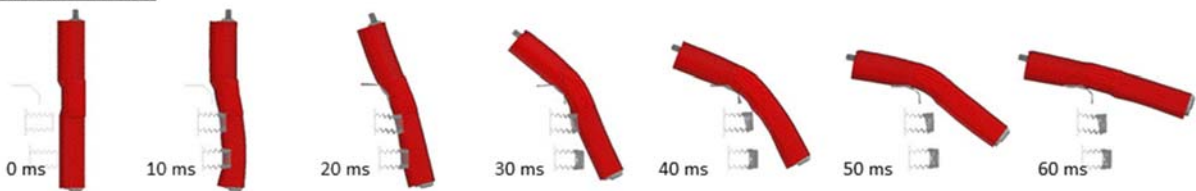


Fig. 14. Evaluation results of the aPLI PT actual test tool compared with human full-body FE model and FlexPLI FE model (kinematics, low-bumper type collision).

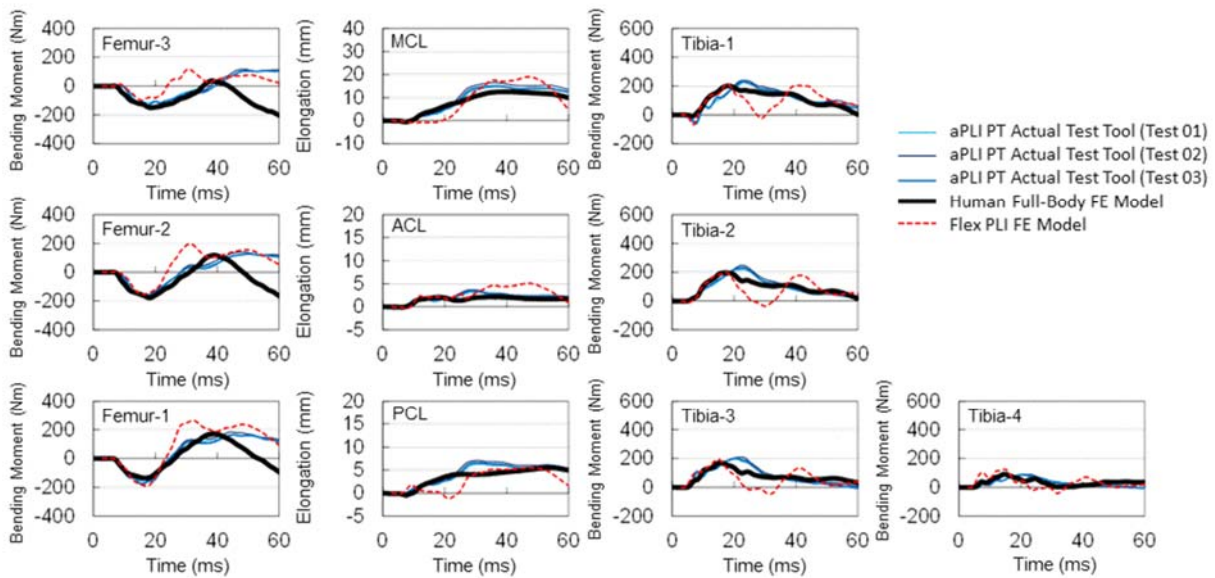
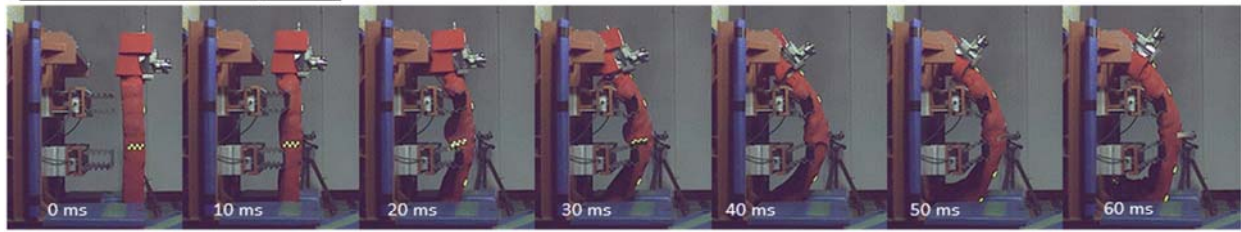
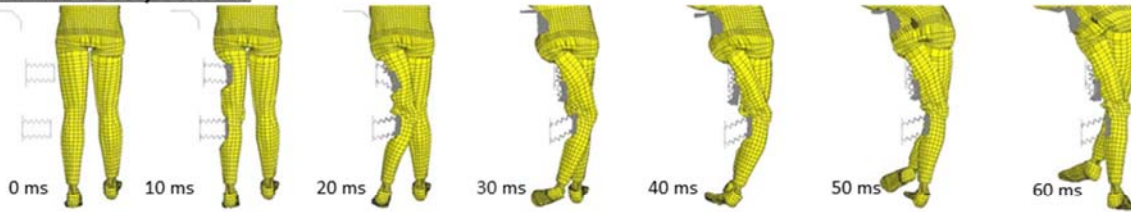


Fig. 15. Evaluation results of the aPLI PT actual test tool compared with human full-body FE model and FlexPLI FE model (Injury measures, low-bumper type collision).

aPLI PT Actual Test Tool (Test 04)



Human Full-Body FE Model



Flex PLI FE Model

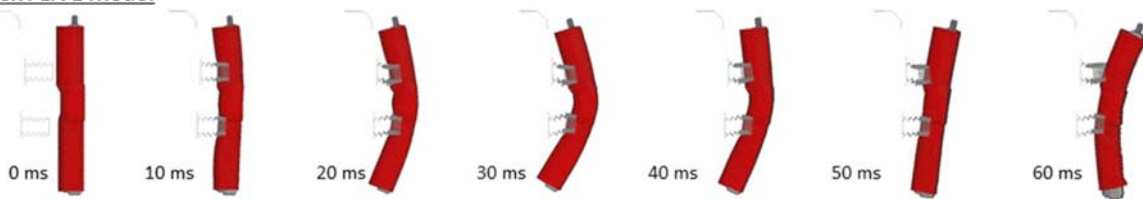


Fig. 16. Evaluation results of the aPLI PT actual test tool compared with human full-body FE model and FlexPLI FE model (kinematics, high-bumper type collision).

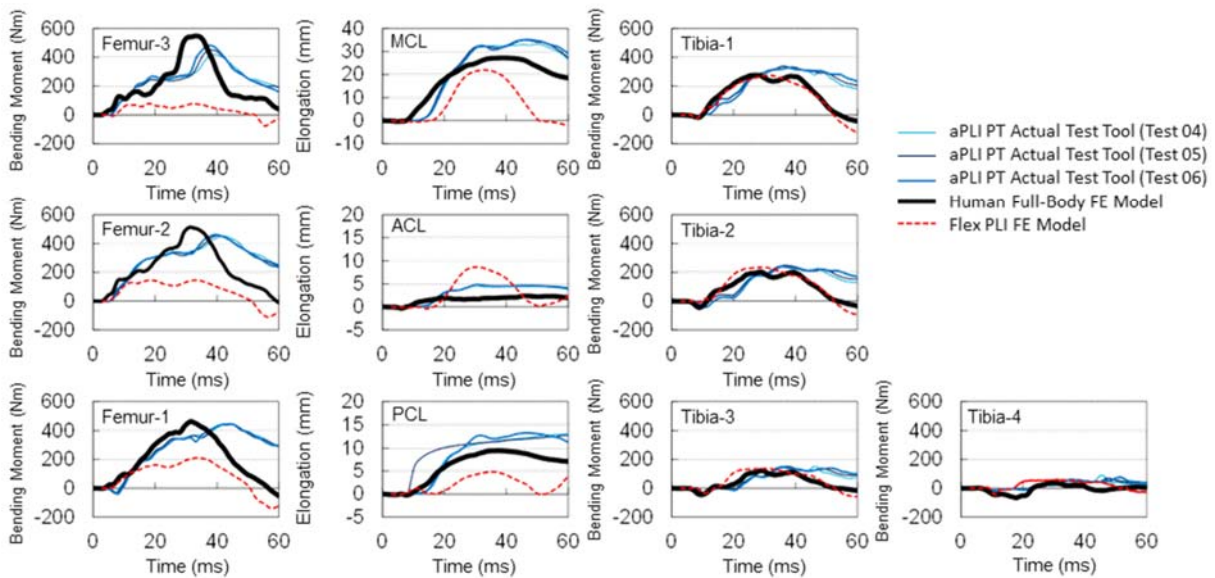


Fig. 17. Test results of the aPLI PT actual test tool compared with human full-body FE model and FlexPLI FE model (injury measures, high-bumper type collision).

#### IV. DISCUSSION

We developed the aPLI PT actual test tool based on its FE model. It shows comparable responses under the component tests for tibia, knee, and femur. On the other hand, with regard to the hip joint, its characteristics show some differences compared to those of the FE model because of the softness of the urethane springs or sticking phenomenon in its housing. We evaluated those influences by developing an aPLI PT FE model which has comparable hip joint characteristics that of an actual test tool (aPLI PT FE Model - RevH, Appendix Figure A-3). Then, we confirmed those influences are relatively small under the simplified vehicle impact test conditions with a low-bumper and high-bumper (Appendix Figure A-4 to Figure A-6). However, if we can find a better solution to simulate the hip joint characteristics of the aPLI PT FE model using other spring material or systems or better construction, it would be preferable.

Under the free flight tests to the actual simplified vehicles (low-bumper and high-bumper), we confirmed no technical issues exist with regard to free flight attitude, vibration, and its durability. In addition, we confirmed its high biofidelity under collisions with the actual simplified vehicles. Therefore, even if we need to make some modifications to the hip joint characteristics to obtain better biofidelic performance, this research demonstrated that we are able to develop an actual test tool of an advanced pedestrian legform impactor which can be applicable to all types of vehicles regardless of the bumper height without any serious technical feasibility issues.

On the other hand, the aPLI PT has a complicated construction compared to that of the FlexPLI in order to improve its biofidelity. In addition, the total mass of the impactor increased by approximately 20 kg compared to that of the FlexPLI because of adding the aPLI PT SUBP part to simulate the upper body influence of the pedestrian. This causes more difficulty in setting the impactor because of the heavy weight, and requires higher launching energy for the free flight test.

Therefore, in our development of the aPLI prototype 2 (aPL PT-2) in the near future, we are going to clarify the best balanced specifications for the aPLI PT-2 considering biofidelity, simplicity, as well as total mass.

#### V. CONCLUSIONS

In this study, we developed an advanced pedestrian legform impactor prototype actual test tool based on its FE model. As a result, we confirmed no serious technical issues to fabricate it as an actual test tool as well as to conduct free flight tests using it. In addition, we confirmed its high biofidelity under free flight tests against low-bumper and high-bumper actual simplified vehicles.

Even if we need to consider further improvement of the fidelity of the hip joint characteristic against those of the FE model to improve its biofidelic performance, through this research, we demonstrated that we are able to fabricate an advanced pedestrian legform impactor actual test tool and using it under free flight test condition without any serious technical feasibility issues.

#### VI. REFERENCES

- [11] Isshiki T, Konosu A, Takahashi Y. Development and Evaluation of the Advanced Pedestrian Legform Impactor Prototype which can be Applicable to All Types of Vehicles Regardless of Bumper Height - Part 1: Finite Element Model -. *Proceedings of IRCOBI Conference*, 2016, Malaga (Spain).
- [12] E/ECE/324/Rev.2/Add.126/Rev.1-E/ECE/TRANS/505/Rev.2/Add.126/Rev.1, Regulation No. 127 (01 series of amendments to the Regulation – Date of entry into force: 22 January 2015). Internet: [<http://www.unece.org/fileadmin/DAM/trans/main/wp29/wp29regs/updates/R127r1e.pdf>], Date Updated [10 June 2016].

VII. APPENDIX

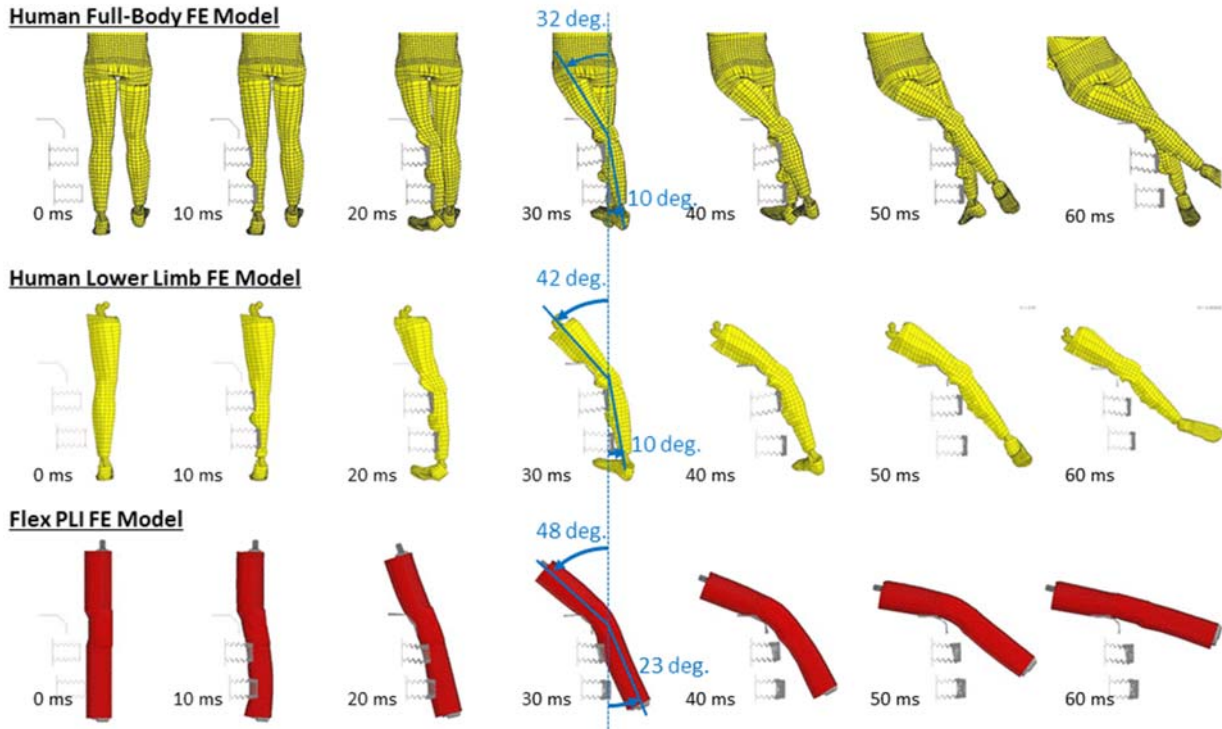


Fig. A-1. Simulation results under collisions with the Low-Bumper type actual simplified vehicle (the human lower limb FE model and the FlexPLI FE model shows a larger lean down phenomenon).

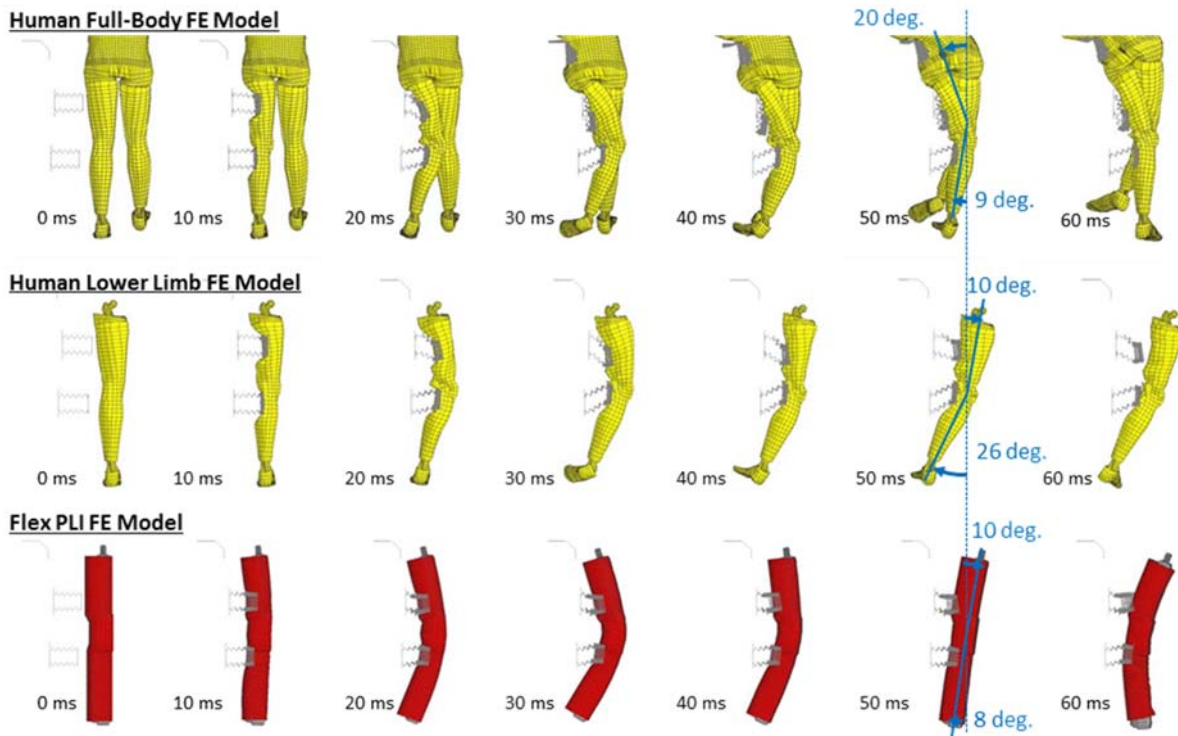


Fig. A-2. Simulation results under collisions with the High-Bumper type actual simplified vehicle (the human lower limb FE model and the FlexPLI FE model show significant rebound phenomenon).

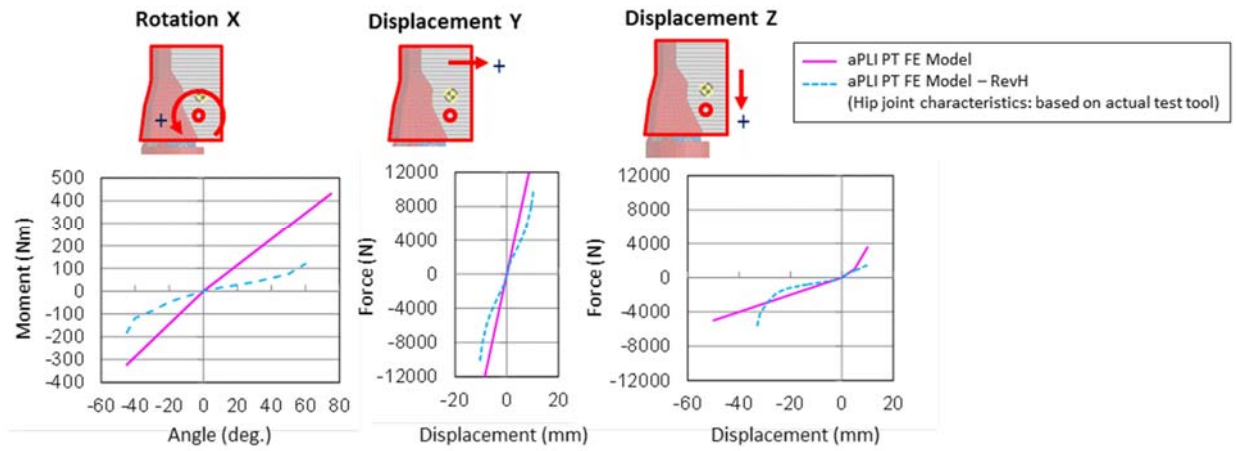


Fig. A-3. Hip joint characteristics (aPLI PT FE model and aPLI PT FE model - RevH).

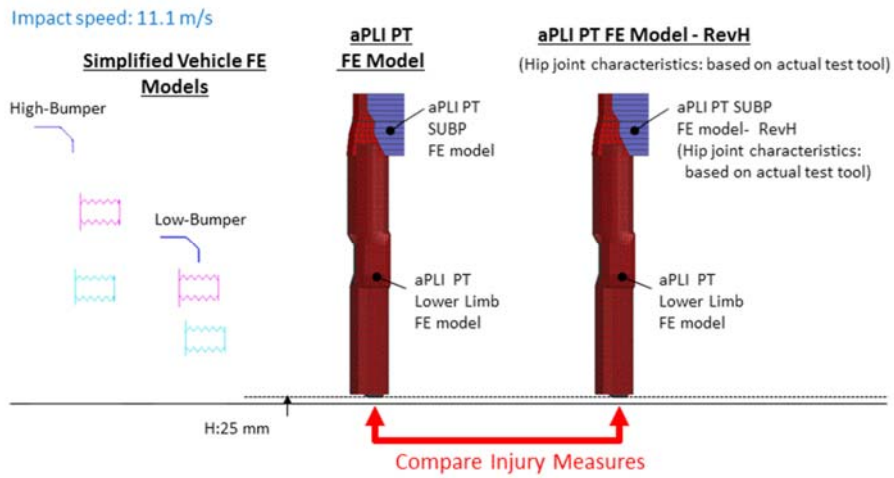


Fig. A-4. Overview of the CAE analysis on the influence of the hip joint characteristics.

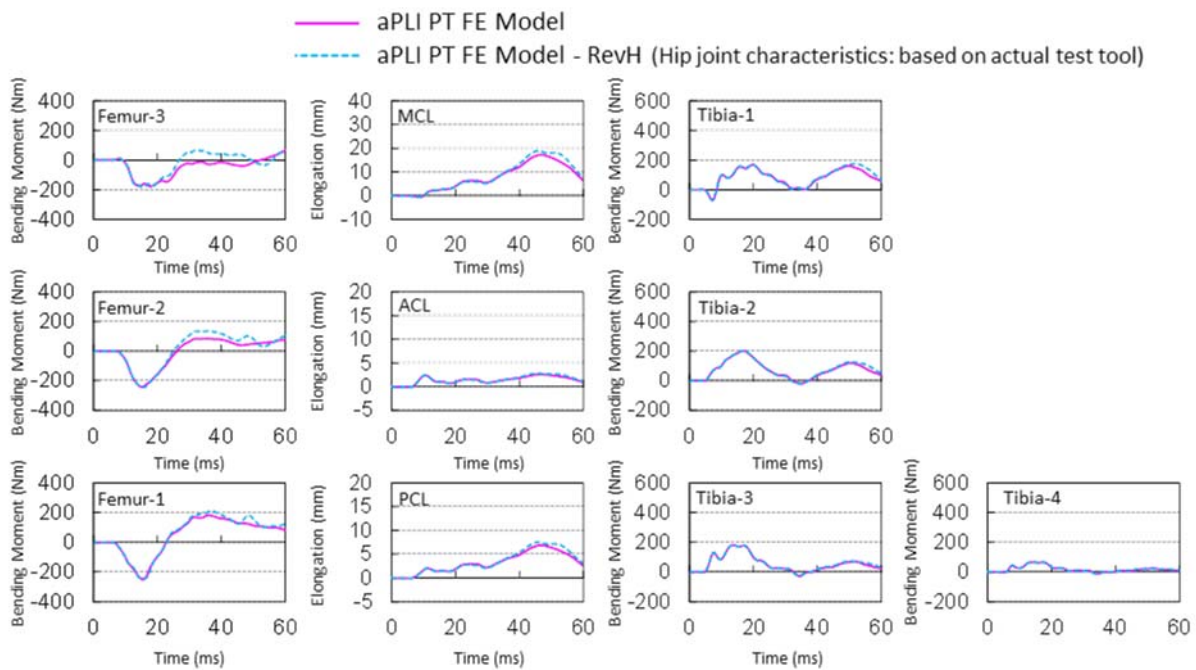


Fig. A-5. Influence of the hip joint characteristics under the collision with the simplified vehicle FE model (injury measures, low-bumper).

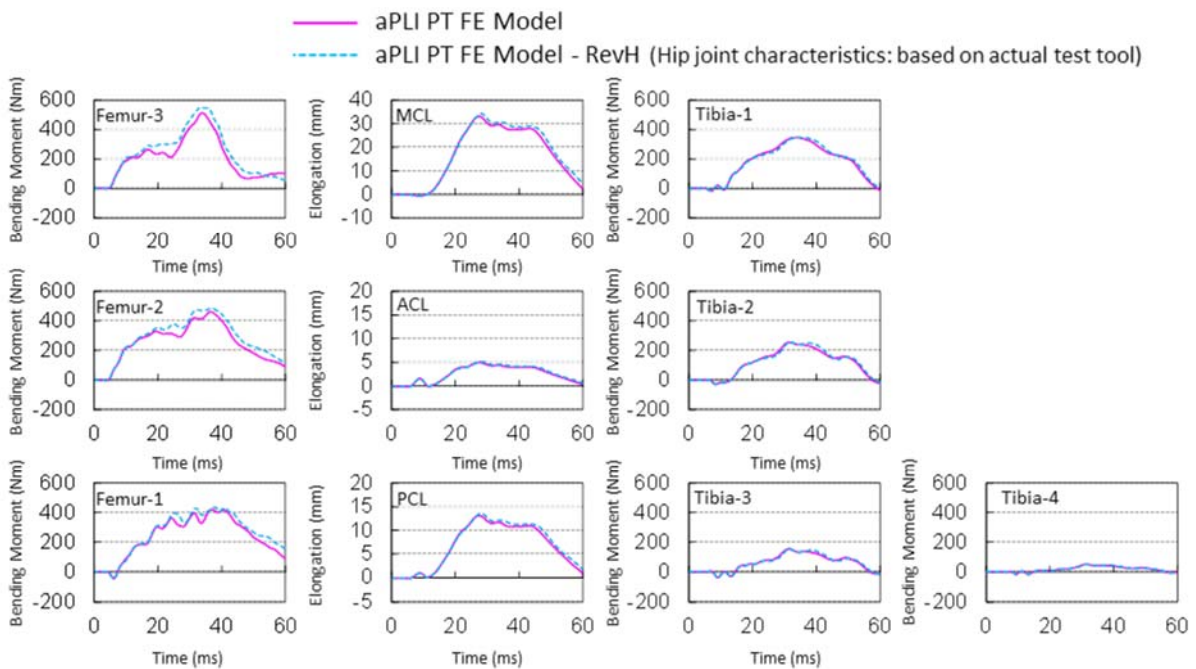


Fig. A-6. Influence of the hip joint characteristics under the collision with the simplified vehicle FE model (injury measures, high-bumper).